J Mater Sci (2010) 45:3058–3066
DOI 10.1007/s10853-010-4312-z

Mechanical characteristics of pure Mg and a Mg/Y_2O_3 nanocomposite in the 25–250 °C temperature range

Ashis Mallick · Khin Sandar Tun · Srikanth Vedantam · Manoj Gupta

Received: 9 October 2009 / Accepted: 9 February 2010 / Published online: 23 February 2010

Abstract In this study, the effect of nano-yttrium oxide particles on the mechanical properties of pure magnesium at elevated temperatures is investigated. Mg/Y_2O_3 (2 wt%/0.7 vol%) bulk composite was synthesised via a powder metallurgy technique incorporating microwave sintering and hot extrusion. Tensile properties and Brinell hardness behavior of pure Mg and composite samples in the 25–250 °C temperature range were investigated. Both tensile and yield strengths of pure Mg and Mg/Y_2O_3 composite samples decreased with an increase in testing temperature. The elongation to failure, however, increased up to 200 °C. At all temperatures, the overall mechanical response of the composite samples was found to be superior compared to pure magnesium and this is primarily attributed to the presence of Y_2O_3 particles in the magnesium matrix.

Introduction

Magnesium alloys and composites are gaining significant attention in diverse engineering sectors primarily due to their light weight, high specific strength, excellent damping, and machinability [1–3]. Because magnesium is one of the lightest (density $\sim$ 1.74) metallic materials it has great potential in structural applications in aerospace, automotive, electronics, sports, and space sectors. However, the low ductility of Mg-based materials—arising from the paucity of slip systems in hexagonal closed packed (HCP) structures—has often restricted their use in engineering applications. In order to enhance the ductility, Mg and its alloys have been reinforced by Al_2O_3 [4], Ti [5], CNTs [6], and SiC [7]. Furthermore, Mg and its alloys are highly temperature sensitive and a rapid degradation of mechanical properties, especially in strength, is observed at elevated temperatures [8, 9]. Many industrial applications of magnesium and its alloys require operation at elevated temperatures [10, 11]. Due to their low melting points (around 650 °C), Mg and its alloys often start losing their strength at temperatures as low as 90 °C making them unsuitable for many applications that require certain threshold strength at higher temperatures. In recent studies [12, 13], investigators have reported that a good combination of strength, hardness, and ductility can be achieved at moderately elevated temperatures using ceramic reinforcement particles in the Mg matrix. In a recent study, Tun et al. [14] demonstrated that tensile response of pure magnesium at ambient temperature can be improved by the addition of nanosized Y_2O_3 particles. However, to the best of our knowledge, there have been no studies of the elevated temperature mechanical properties of Mg/Y_2O_3 nanocomposites prepared by an energy efficient microwave-assisted sintering process.

Accordingly, the main focus of this study was to study the effect of increasing temperature on the mechanical behavior of pure magnesium and a magnesium nanocomposite in which 2 wt% nano-Y_2O_3 particles were used as reinforcement. Tensile and Brinell hardness tests were conducted on Mg and Mg/Y_2O_3 samples in 25–250 °C temperature range. Particular emphasis was placed on the effect of Y_2O_3 particles on the mechanical response in comparison with pure magnesium as a function of temperature.

A. Mallick · K. S. Tun · S. Vedantam · M. Gupta (✉)
Department of Mechanical Engineering, National University of Singapore, 9 Engineering Drive 1, Singapore 117576, Singapore
e-mail: mpegm@nus.edu.sg

Experimental procedures

Materials

Pure commercial magnesium powder of 98.5% purity with an average particle size of 60–300 μm (Merck, Germany) was used as the matrix material. As the ceramic reinforcement phase, Y_2O_3 was chosen due to its potential to strengthen the Mg. In this study, nanosized (30–50 nm) yttrium oxide (Inframat Advanced Materials, USA) powder was used. Y_2O_3 also displays high thermal stability up to its melting temperature (~2,690 °C) together with superior resistance to aggressive chemical attack, erosion, and thermal shock. High thermal stability of yttrium oxide suggests minimal reaction between matrix and reinforcement leading to good interfacial integrity [15]. Based on the results of an earlier study [14], we only considered alloys of 2 wt% Y_2O_3.

Processing

Magnesium reinforced with 2 wt% Y_2O_3 nanoparticles was synthesized by a powder metallurgy technique. Micron size powder of Mg and nanopowder of Y_2O_3 were weighed carefully in an air controlled electronic weighing machine (Mettler Toledo, Model no.: AB30-S, Switzerland) having an accuracy up to 1.0 μg. The mixture of weighed powders was then shaken carefully inside the sealed plastic container followed by blending to obtain a uniform composition of the resultant composite. The blending was done in a RETSCH PM-400 mechanical alloying (MA) machine for 1 h. The machine was operated at 200 rpm in both clockwise and counterclockwise directions. No balls or process control agents were used during the blending step. After blending, the mixture of Mg and Y_2O_3 powders was placed in a hollow cylindrical die and cold compacted using an isostatic pressure of 97 bar (50 tons) to produce a cylindrical billet of 35-mm diameter and 40-mm height. The compacted cylindrical billets were then spray-coated with colloidal graphite for sintering. The graphite coating is necessary to protect the Mg from oxidation during the sintering process. The sintering was carried out in a microwave oven (SHARP 900 W, 2.45 GHz), and the sintering process involved heating to 640 °C followed by cooling. Finally, the sintered billets were hot extruded to obtain a 7-mm diameter cylindrical rod. The extrusion was carried out at 350 °C temperature with an extrusion ratio of 25:1 using a 150-ton hydraulic press. Prior to extrusion, the sintered billets were soaked at a temperature of 400 °C for 1 h. Pure Mg rods were prepared using a similar procedure as discussed above except that blending step was not used.

Microstructural characterization

Microstructural characterization was carried out on metallographically polished reinforced and unreinforced samples using a standard metallographic approach. The characterization procedure included the investigation of grain size, grain morphology, presence of porosity, and distribution of reinforcement. The fracture morphology at room temperature and at elevated temperatures (150 and 250 °C) for pure Mg and composite samples was also studied. The analyses were performed using HITACHI S-4300 field emission scanning electron microscope (FESEM), and an OLYMPUS metallographic optical microscope and Scion Image Analyzer.

X-ray diffraction analysis

To identify the constituent phases and to analyze the texture changes in pure Mg and the composite, X-ray diffraction (XRD) analysis was carried out on the polished extruded samples and the samples deformed at 250 °C. An automated Shimadzu LAB-X-6000 X-ray diffractometer with Cu Kα radiation ($\lambda = 1.5406$ Å) was used. The machine was operated at 30 kV and 40 A with a scanning speed of 2°/min.

Mechanical characterization

The mechanical characteristics of pure Mg and Mg/Y_2O_3 nanocomposite were evaluated in terms of hardness and tensile properties. A computer controlled universal material testing machine (*Model:* Instron 8874) with load-cell of 25 kN and sensitivity of 5 N was used for both the hardness and tensile testing. A digitally controlled resistance heating environmental chamber (accuracy of ±1 °C) was attached to the testing machine. Tests were conducted at temperatures of 25, 100, 150, 200, and 250 °C. Prior to testing, the specimens were soaked for 15 min at the intended temperatures to realize temperature homogeneity.

To perform tensile testing, 7-mm diameter extruded rods were machined into tensile specimens of 5 mm gauge diameter and 25 mm gauge length in accordance with ASTM standard E8 M-01. The cross-head speed of the load-cell was chosen to be 0.254 mm/min throughout the tests. Four tests were performed at each test temperature. Stress–strain curves at all test temperatures were obtained from the tensile test data, and the work of fracture values were also computed using a simple mathematical conversion of these data.

For measuring hardness at different temperatures, the extruded bulk cylindrical specimens of 7 mm diameter and 7 mm height were polished using a 10-μm polishing cloth. A compressive load was applied through a spherical ball of 5-mm diameter (made of hard stainless steel) and

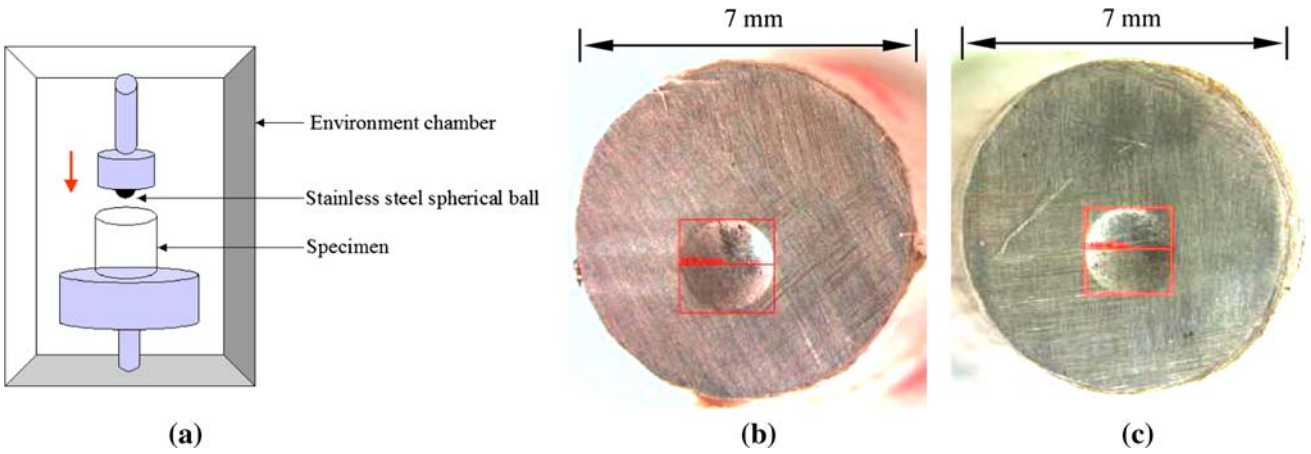

Fig. 1 Representation of **a** experimental setup for Brinell hardness test, **b** pure Mg sample after indentation at room temperature, and **c** nanocomposite sample after indentation at room temperature

indentation rate (0.1 mm/min) and the maximum load was carefully maintained through computer control. To avoid excessive indentation, the maximum applied load for the indentation was set at 1,000 N and the holding time was set to 20 s. The schematic diagram of experimental setup and the indentations made are shown in Fig. 1. No change in overall dimensions of the samples was observed following indentation tests.

Fracture behavior

A scanning electron microscope (SEM) was employed to examine the fracture surfaces of the tensile specimens immediately after the tensile test so as to prevent oxidation of the fracture surfaces. Fractographic analysis of unreinforced and reinforced samples was carried out to gain insight into fracture mechanism of samples tested at room and elevated temperatures.

Results and discussion

Synthesis of Mg/2 wt% Y_2O_3 nanocomposite

The pure Mg and Mg/2 wt% Y_2O_3 nanocomposite were synthesized using a powder metallurgy technique incorporating a microwave-assisted hybrid sintering process and hot extrusion. Microwave-assisted sintering enabled the reduction of the sintering time from 3 h to only 13 min for the present nanocomposite leading to a reduction of ~93% of sintering time.

Microstructural characterization

Figure 2 shows the typical microstructures of extruded Mg/Y_2O_3 nanocomposite (a) and (c), pure Mg (b) and the deformed nanocomposite (d). The micrograph of the deformed sample represented here was tested (tensile) at temperature of 250 °C. Relatively well-distributed nanosized Y_2O_3 particles with a few clusters and nanopores were observed in the FESEM micrograph of the extruded composite sample (Fig. 2a). The grain size and aspect ratio of the extruded pure Mg and its composite are shown in Table 1. The grain size measurement shows the reduction in average matrix grain size in the composite sample. Considering the standard deviation, the variation in grain size can be considered insignificant. The inability of nanosized Y_2O_3 particles to restrict the grain size can be attributed to their low volume fraction. The low porosity levels exhibited by the pure Mg and Mg/Y_2O_3 composite materials (Fig. 2a, Table 1) indicate the suitability of the processing methodology and parameters in ensuring near dense monolithic and composite samples. These results are consistent with observations made in earlier studies [16, 17].

X-ray diffraction analysis

Figure 3 shows the XRD diffractograms of the pure Mg and nanocomposite samples. XRD profiles of the undeformed samples are compared with that of the samples deformed after tensile testing at 250 °C. It was observed that Mg is the dominant phase from all the XRD diffractograms. The appearance of Y_2O_3 (2 2 2) peak can be seen at 29.15° in the XRD spectrum of nanocomposite (Fig. 3b). The absence of MgO or any other related phases of Mg in the deformed samples (monolithic and composite) indicates the absence/minimal presence of MgO and absence/extremely limited decomposition of Y_2O_3 during tensile testing at high temperatures. Both these events cannot be completely ruled out due to the limitation of XRD technique to detect the phases below 2 vol% [18]. However,

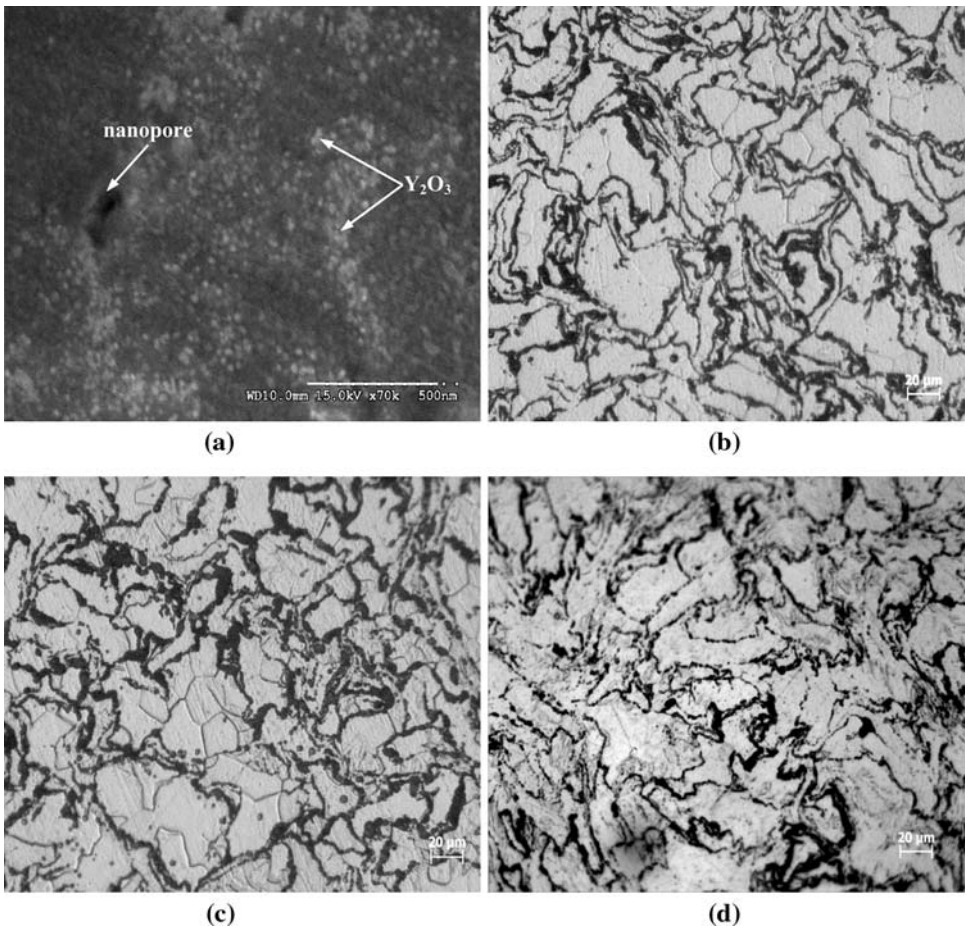

Fig. 2 Representative micrographs showing **a** distribution of nano-Y_2O_3 particles and the presence of nanopores in the bulk extruded composite sample, **b** microstructure of monolithic Mg, **c** nanocomposite, and **d** microstructure of deformed tensile specimen of nanocomposite after its fracture at 250 °C

Table 1 Results of density, porosity, and grain morphology determination of Mg and Mg/Y_2O_3

Material	Density (g/cc)		Porosity (vol%)	Grain morphology	
	Theoretical	Experimental		Size (μm)	Aspect ratio
Mg	1.740	1.738 ± 0.007	0.13	20 ± 3	1.4 ± 0.1
Mg/2% Y_2O_3	1.763	1.757 ± 0.006	0.35	18 ± 3	1.4 ± 0.2

the results do indicate the efficacy of microwave-assisted powder metallurgy technique to minimize or eliminate reaction between matrix and reinforcement and between matrix and ambient environment. Further work using the technique of transmission electron microscopy is required to establish the feasibility of above reactions during the synthesis route adopted in this study and during testing at high temperatures. A reduction in intensity of Mg (0 0 0 2) peak in the extruded composite sample was observed when compared to pure Mg. The possible reason may be the presence of reinforcement that facilitated the rotation of basal plane of Mg preferentially in the direction of [1 0 −1 1] during extrusion [19]. This indicates that composite samples exhibit stronger basal texture (fiber texture) when compared to pure Mg. This is also the reason for obtaining higher yield strength in the composite samples than that of pure Mg. The presence of strong basal texture in the composite sample limits basal slip activation which could provide higher yield strength. The observed relation between texture and yield strength for this study is consistent with the previous study [20]. Since the basal planes are mostly aligned parallel to the extrusion direction, it could favor the activation of non-basal slip providing higher ductility in the composite sample. After tensile deformation at 250 °C, the intensity of the (0 0 0 2) diffraction peak increased at the expense of the (1 0 −1 0) peak in the case of the composite sample, which shows that the basal planes are mostly aligned perpendicular to the tensile axis. In contrast, the reduction of the (0 0 0 2) peak with an increase in intensity of the (1 0 −1 0) peak was observed in pure Mg. This indicates the inclination of some basal planes at an angle (not perpendicular) with respect to tensile axis. Previous studies [21–23] have reported that ductility can be increased in accordance with the favorable basal slip activation if the basal planes align ∼45° to extrusion axis or misalign from the extrusion axis. The

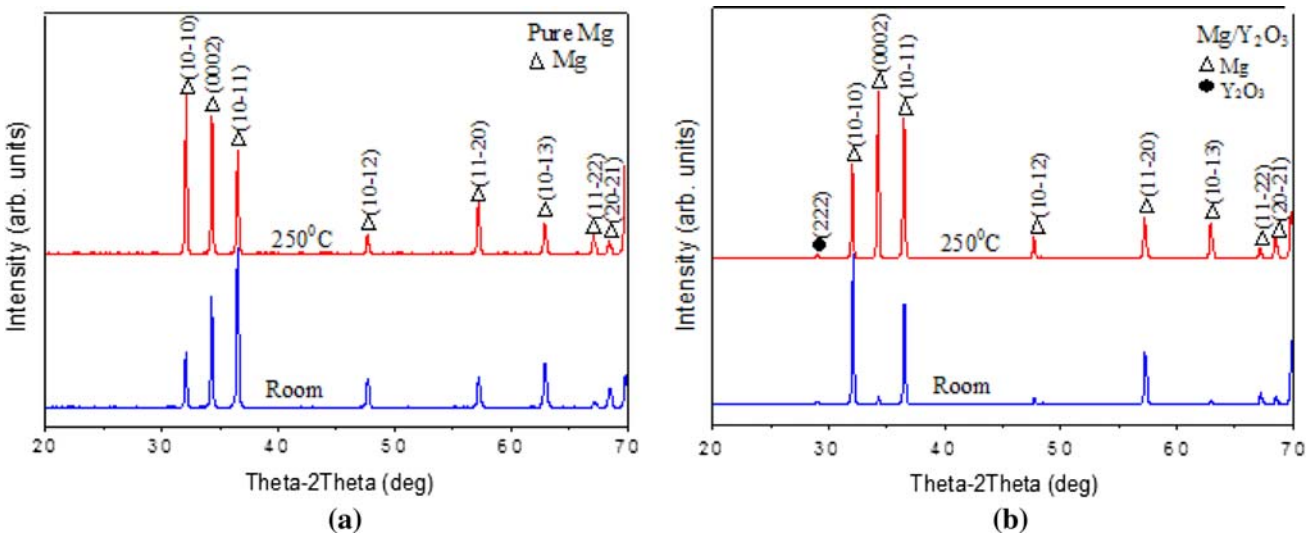

Fig. 3 XRD spectra of **a** pure Mg and **b** Mg/Y_2O_3 nanocomposite

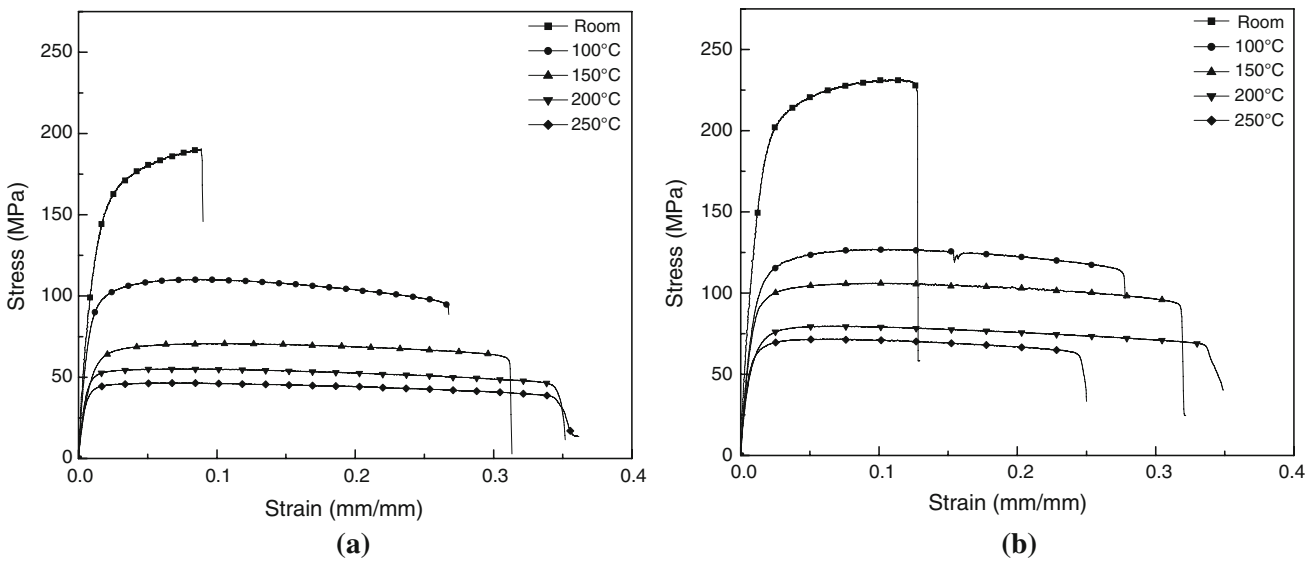

Fig. 4 Comparison of engineering stress–strain curves at various temperatures for **a** pure Mg and **b** Mg/Y_2O_3 nanocomposite

current result of an increased strain to fracture observed in pure Mg when compared to the composite sample at 250 °C is in agreement with the above-mentioned studies (Fig. 4).

Mechanical characterization

Figure 4 shows the engineering stress–strain curves of the pure Mg and Mg/Y_2O_3 nanocomposite samples tested in the 25–250 °C temperature range. In both cases, the nature of loading curves after yielding was different at high temperatures when compared to that of room temperature. Work hardening after yielding was observed when both pure and composite samples were tested at room temperature, whereas hardening followed by a little softening was observed in the samples tested at higher temperatures. The near flat character from the flow curves beyond the yield point can be characterized as almost perfect elastic–plastic behavior. The variations in yield strength (0.2% YS) and ultimate tensile strength (UTS) of the composite as a function of temperature are compared to that of matrix material in Fig. 5. The data points represent the average value of four tests, and the error bars represent the standard deviation in each case.

At every test temperature (25–250 °C), the strength of the composite samples was found to be higher than that of

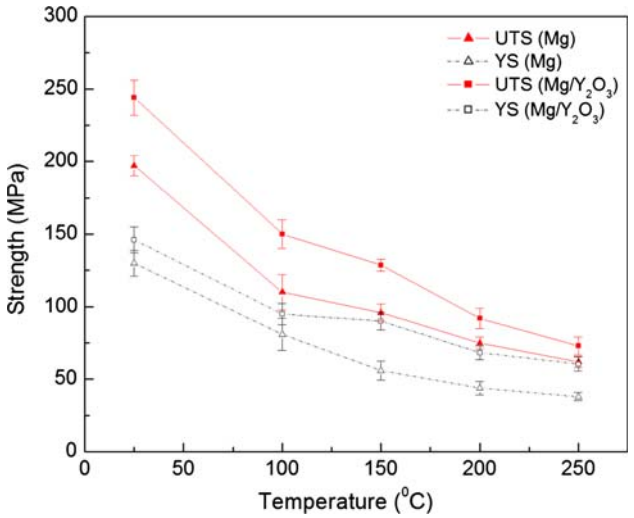

Fig. 5 Variation of the yield strength (0.2% YS) and ultimate tensile strength (UTS) as a function of test temperatures for pure Mg and Mg/Y_2O_3 nanocomposite

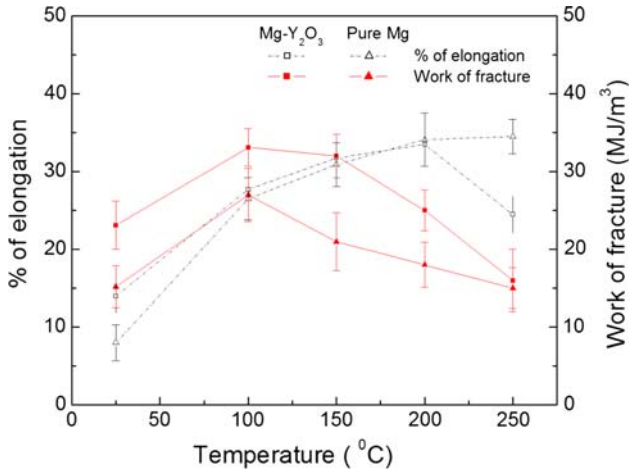

Fig. 6 Variation of the failure strain and work of fracture as a function of test temperatures for pure Mg and nanocomposite

pure Mg (Figs. 4, 5). At room temperature, the strengthening mechanisms of the composite can be described by the Orowan mechanism, interface strengthening, and cold deformation hardening mechanisms due to the presence of yttria nanoparticles in Mg matrix [14]. At temperature ≥150 °C, however, Orowan and interface strengthening are expected to play a major role. With increasing test temperature, a decreasing trend of both yield and ultimate tensile strengths was observed in both Mg and Mg/Y_2O_3 nanocomposite. A rapid drop in yield and ultimate tensile strengths was observed when the test temperature was raised from 25 to 100 °C in both pure material and the composite. Above 100 °C and up to 250 °C, strength decrement was gradual, and this behavior was more prominent in the case of the composite sample (Fig. 4). It can also be seen that the 0.2% YS and UTS in Mg and composite appear to converge with the increasing test temperature (minimal difference in strengths). This can be attributed to a change in dislocation movement mechanism [24]. Similarly a decrease in the strength of both the pure and composites samples indicates a thermally activated plastic deformation response for both samples with an increase in test temperature despite a quantitative difference in the strength (Figs. 4, 5). Thermal activation during the high temperature tensile test causes easy movement of dislocations in the materials leading to reduced applied stress required to support deformation. Even for the composite sample, thermal activation can aid dislocations in readily bypassing barriers arising from second phase particles (yttria) without interacting strongly with them [25]. Although an increase in thermal activation energy due to the applied high temperature reduces the strength, the strength becomes independent of the temperature beyond a critical temperature [25]. This may be the reason for the smaller difference in strength at the higher test temperatures, 200 and 250 °C.

The variation in strain to fracture measured by the percentage elongation and work to fracture as a function of test temperature of the nanocomposite are compared with that of pure Mg in Fig. 6. A gradual increase in strain to fracture with increasing test temperature was observed in both samples (except composite at 250 °C). At room temperature, higher strain to fracture was observed in the nanocomposite as compared to Mg matrix material. However, similar level of strain to fracture for pure Mg and the nanocomposite was observed at elevated test temperatures up to 200 °C. At room temperature, the presence of yttria nanoparticles in the Mg matrix could help to activate non-basal slip and cross slip tendency in promoting strain to fracture of the composite [14]. It is well known that non-basal slip systems are operative even for pure Mg at high temperatures, resulting in high strain to fracture [26]. It is thus evident from the current results that the role of yttria as a possible non-basal slip activator was dominated by the usual phenomenon of temperature-dependent non-basal slip evolution. Figure 7 shows the deformed samples of pure Mg and nanocomposite tested at various temperatures. It can be seen that onset of necking does not occur even after high temperature tensile testing which implies that uniform deformation continued until sharp decrease of load at every test temperatures (Figs. 4, 7).

Hardness measurements

The results of Brinell hardness at various temperatures of pure Mg and its composite are compared in Table 2. The values were calculated from the following empirical relation [27]:

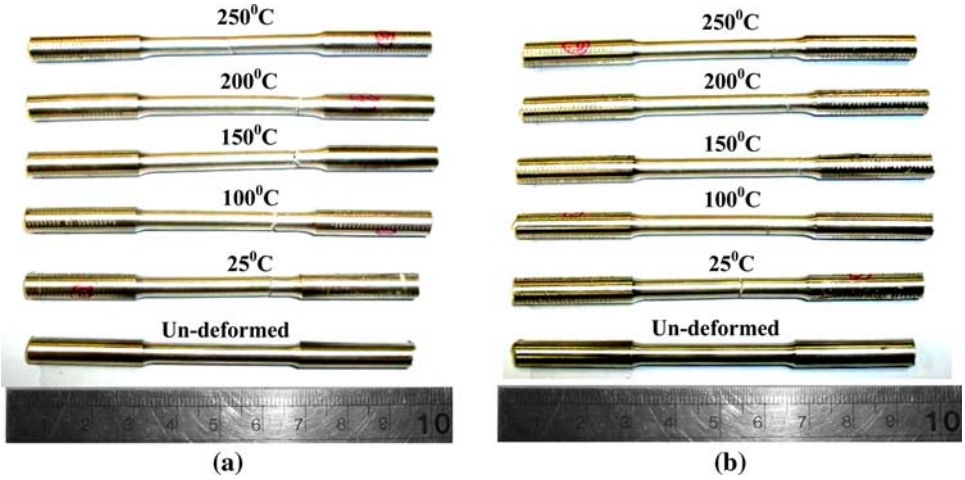

Fig. 7 Deformed tensile specimen of **a** pure Mg and **b** nanocomposite tested at various temperatures

Table 2 Variation of Brinell hardness as a function of temperature for pure Mg and Mg/Y_2O_3 nanocomposite

Material	Brinell hardness (in MPa) at various temperatures				
	25 °C	100 °C	150 °C	200 °C	250 °C
Pure Mg	306	202	134	101	88
Mg/2.0% Y_2O_3	371	247	219	197	162

$$\mathrm{BH} = \frac{2P}{\pi D\left(D - \sqrt{(D^2 - d^2)}\right)} \quad (1)$$

where P is the applied load, D is the diameter of spherical ball, and d is the diameter of indentation. The composite samples showed higher value of hardness when compared to pure Mg at every test temperature. These results revealed that nanosized Y_2O_3 reinforcement in a Mg matrix is effective in increasing the resistance to localized plastic deformation [28]. With increasing test temperature, a decreasing trend in hardness was observed in both unreinforced and reinforced samples. This phenomenon is natural as with an increase in test temperature, the material is expected to be softened due to thermal expansion. However, a lower softening rate about 30 MPa/50 °C was observed in the composite as compared to pure Mg. This may be attributed to the pinning effect of nano-Y_2O_3 particles in composite matrix [24] as well as the lower coefficient of thermal expansion (CTE) of Mg/2 wt% Y_2O_3 as compared to Mg [14]. The relationship between the hardness and test temperature was fitted to the simple exponential power law as [29]

$$H = Ae^{-BT}, \quad (2)$$

where H is the measured hardness in MPa, T is temperature in Kelvin and A and B are the material constants. The fitting of hardness–temperature plot (Fig. 8) gives a negative slope

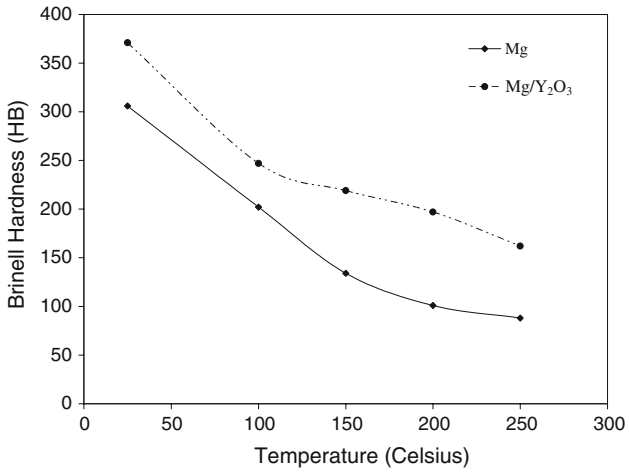

Fig. 8 Variation of Brinell hardness as a function of test temperatures in pure Mg and Mg/Y_2O_3 nanocomposite

which is in agreement with the hardness–temperature relationship.

Fracture behavior

Figure 9 represents the fracture topographies of pure Mg and Mg/Y_2O_3 composite tested at room temperature and at 150 and 250 °C. The fracture surface of pure Mg sample deformed and failed at room temperature shows brittle fracture characteristics [30] with a visible microscopic rough surface (see Fig. 9.i.a) while that of fractured samples at 150 and 250 °C shows more evidences of plastic deformation (see Fig. 9.ii.a, iii.a). This phenomenon supports the enhanced deformability of the samples tested at high temperatures. On the other hand, at room temperature, the composite failed in a mixed mode fracture as evidenced by a few dimple-like features in the fracture surfaces (see Fig. 9.i.b). The presence of dimples on the fractured surface of hexagonal-close-packed magnesium indicates its

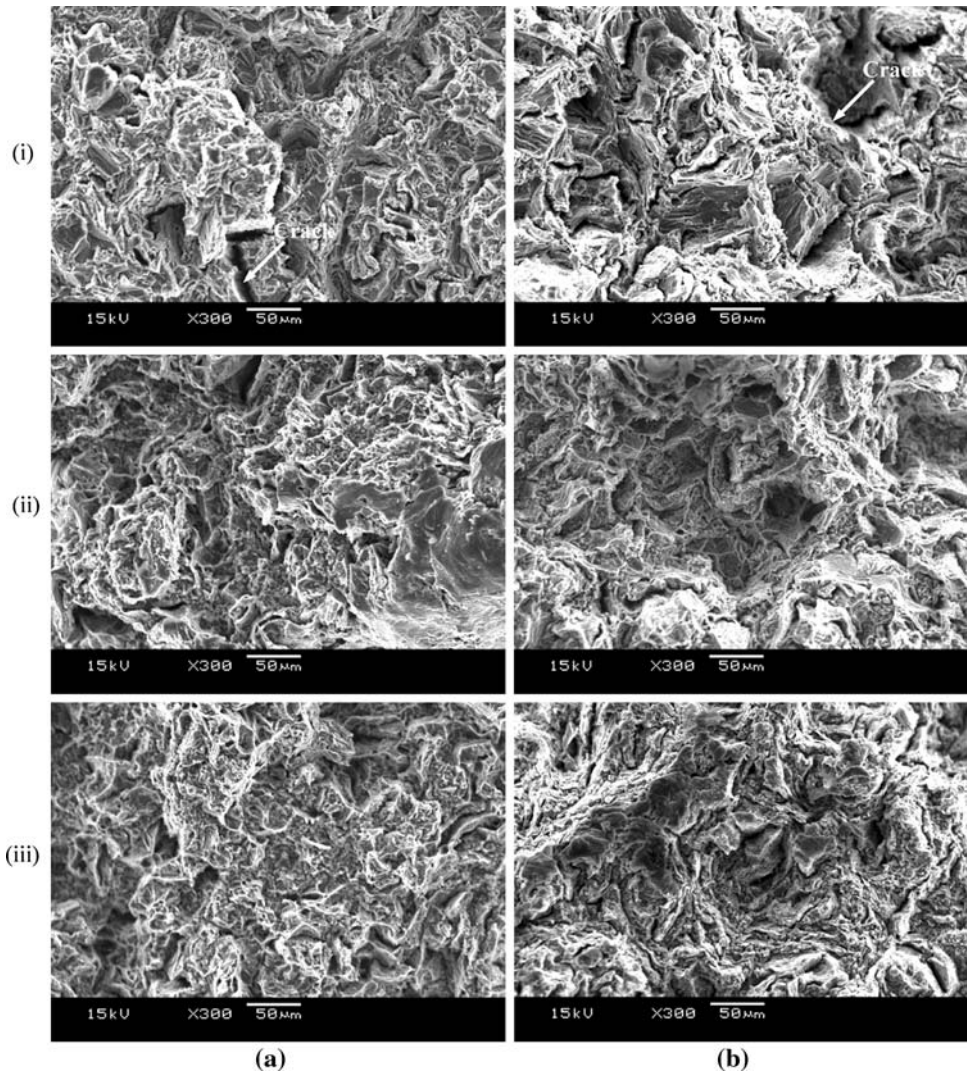

Fig. 9 Tensile fracture surfaces of **a** pure Mg and **b** nanocomposite tested at (i) room temperature, (ii) 150 °C, and (iii) 250 °C

enhanced deformability. It is also to be noted that the non-basal (prismatic) slip system was activated (from XRD result) at room temperature (25 °C) due to the reinforcement of nanosized Y_2O_3 in Mg matrix leading to improved ductility exhibited by the composite samples. The results of fracture surface characterization are consistent with the results of tensile testing discussed earlier.

Conclusions

This study reported the elevated temperature mechanical properties of pure Mg and Mg matrix reinforced with nanosized Y_2O_3 particles. From this study, the following conclusions can be drawn:

1. Mg/Y_2O_3 nanocomposite showed reasonably uniform distribution of yttria in Mg matrix which assisted in the improvement of yield and ultimate tensile strengths of composite when compared to pure Mg irrespective of test temperatures.
2. A superior yield and ultimate tensile strength was exhibited by Mg/Y_2O_3 nanocomposites when compared to pure Mg at every test temperature (25–250 °C). Similarly a decrease of strength with increasing test temperatures was observed in both pure and composite samples.
3. Strain to fracture of both pure Mg and Mg/Y_2O_3 nanocomposite increased with an increasing temperature. For Mg/Y_2O_3 nanocomposite at 250 °C test temperature, the strain to fracture reduced due to the orientation of basal (0 0 0 2) planes perpendicular to the tensile axis.
4. When compared to pure Mg, the presence of yttria provided strength improvement while strain to fracture was independent of its presence at each test temperature above room temperature.

5. Hardness values were higher in the composite when compared to those of pure Mg at each test temperature while the same decreasing trend of hardness was observed in both with an increase in test temperature.

References

1. Evans A, Marchi CS, Mortensen A (2003) Metal matrix composites in industry: an introduction and a survey. Kluwer, Boston
2. Lu L, Thong KK, Gupta M (2003) Comp Sci Technol 63:623
3. Lukac P, Trojanova Z (2005) Int J Mater Prod Technol 23:121
4. Hassan SF, Gupta M (2004) Mater Sci Technol 20:1383
5. Perez P, Garces G, Adeva P (2004) Comp Sci Technol 64:145
6. Goh CS, Wei J, Lee LC, Gupta M (2006) Nanotechnology 17:7
7. Lu L, Lim CYH, Yeong WM (2004) Comp Struct 66:41
8. Mallick A, Vedantam S, Lu L (2009) Mater Sci Eng A 515:14
9. Avedesian MM, Baker H (1999) Magnesium and magnesium alloys. ASM International, USA
10. Kim YW, Griffith WM (eds) (1988) Dispersion strengthened aluminum alloys. TMS-AIME, Warrendale
11. Fine ME, Starke EA (eds) (1986) Rapidly solidified powder aluminum alloys. ASTM STP 890, ASTM, Philadelphia
12. Hassan SF, Tan MJ, Gupta M (2008) Mater Sci Eng A 486:56
13. Han BQ, Dunand DC (2001) Mater Sci Eng A 300:235
14. Tun KS, Gupta M (2007) Comp Sci Technol 67:2657
15. Thummler F, Oberacker R (1993) An introduction to powder metallurgy. Institute of Materials, London
16. Gupta M, Wong WLE (2005) Scr Mater 52:479
17. Wong WLE, Karthik S, Gupta M (2005) Mater Sci Technol 21:1063
18. Cullity BD (1978) Element of X-ray diffraction, 2nd edn. Addison-Wesley, Reading, p 414
19. Su CW, Chua BW, Lu L, Lai MO (2005) Mater Sci Eng A 402:163
20. Garcés G, Rodríguez M, Pérez P, Adeva P (2006) Mater Sci Eng A 419:357
21. Stanford N, Barnett M (2008) Scr Mater 58:179
22. Agnew SR, Horton JA, Lillo TM, Brown DW (2004) Scr Mater 50:377
23. Goh CS, Wei J, Lee LC, Gupta M (2007) Acta Mater 55:5115
24. Tian B, Liu P, Song K, Li Y, Liu Y, Ren F, Su J (2006) Mater Sci Eng A 435–436:705
25. Smallman RE (1970) Modern physical metallurgy, 3rd edn. Butterworths, London
26. Roberts CS (1960) Magnesium and its alloys. Wiley, New York
27. Callister WD (2003) Materials science and engineering: an introduction, 6th edn. Wiley, New York, p 136
28. Kettunen PO, Kuokkala VT (2002) Plastic deformation and strain hardening. Trans Tech, Enfield
29. Gilman JJ (1973) In: Westbrook JH, Conrad H (eds) The science of hardness and its research applications. ASM, USA, p 54
30. Reed-Hill RE (1964) Physical metallurgy principles, 2nd edn. Van Nostrand Comp., USA